Spectrochimica Acta Part A: Molecular and Biomolecular Spectroscopy 193 (2018) 47–53

Contents lists available at ScienceDirect

Spectrochimica Acta Part A: Molecular and Biomolecular Spectroscopy

journal homepage: www.elsevier.com/locate/saa

Pressure-induced phase transition and fracture in α-MoO_3 nanoribbons

Jose V. Silveira [a],*, Luciana L. Vieira [b], Acrisio L. Aguiar [c], Paulo T.C. Freire [d], Josue Mendes Filho [d,1], Oswaldo L. Alves [b], Antonio G. Souza Filho [d],*

[a] *Departamento de Engenharia da Computação, Universidade Federal do Ceará, Sobral-, CE, Brazil*
[b] *Laboratory of Solid State Chemistry, Instituto de Química – UNICAMP, Campinas, SP, Brazil*
[c] *Departamento de Física, Universidade Federal do Piaui, Teresina, PI, Brazil*
[d] *Departamento de Física, Universidade Federal do Ceará, P. O. Box 6030, CEP 60455-900, Fortaleza, CE, Brazil*

ARTICLE INFO

Article history:
Received 14 August 2017
Received in revised form 16 November 2017
Accepted 25 November 2017
Available online 27 November 2017

Keywords:
Nanomaterial
Hydrostatic pressure
Raman spectroscopy
Phase transition
Molybdenum oxide nanoribbons

ABSTRACT

MoO_3 nanoribbons were studied under different pressure conditions ranging from 0 to 21 GPa at room temperature. The effect of the applied pressure on the spectroscopic and morphologic properties of the MoO_3 nanoribbons was investigated by means of Raman spectroscopy and scanning electron microscopy techniques. The pressure dependent Raman spectra of the MoO_3 nanoribbons indicate that a structural phase transition occurs at 5 GPa from the orthorhombic α-MoO_3 phase (*Pbnm*) to the monoclinic MoO_3-II phase ($P2_1/m$), which remains stable up to 21 GPa. Such phase transformation occurs at considerably lower pressure than the critical pressure for α-MoO_3 microcrystals (12 GPa). We suggested that the applanate morphology combined with the presence of crystalline defects in the sample play an important role in the phase transition of the MoO_3 nanoribbons. Frequencies and linewidths of the Raman bands as a function of pressure also suggest a pressure-induced morphological change and the decreasing of the nanocrystal size. The observed spectroscopic changes are supported by electron microscopy images, which clearly show a pressure-induced morphologic change in MoO_3 nanoribbons.

1. Introduction

Nanostructured materials have attracted great attention of scientific community because this new form allows one to obtain a large range of new properties by exploiting intrinsic (quantum confinement) and/or extrinsic (large area/volume ratio) size-induced effects. Among the different morphologies that materials can be synthesized, particularly interesting is the quasi one-dimensional ones, such as nanotubes, nanorods, nanowires, nanoribbons and nanobelts [1–6]. These nanomaterials usually present size-induced phenomena, which is responsible for emerging interesting and novel properties which depend not only on the crystal structure, but also on the size and morphology of the material. This last phenomenon has opened up several new research directions in quasi one-dimensional materials, including pressure-induced phase and morphology transformations [7–18].

Structural stability and high-pressure behavior of the nanomaterials can be both significantly different from their respective bulk counterparts. The compressibility, phase transition pressures and phase transition routes in nanomaterials can be dramatically modified by the size [7,8], defect ratio [9,10], morphology [11–13], volume expansion [14], exposition and orientation of crystal surface [11,12] and crystal growth direction [15,16]. Although the effect of size and morphology on the properties of several nanomaterials have been well established, up to now, the intrinsic nature of the difference on pressure-dependent behavior of these nanomaterials remains far from being fully understood. In particular, the effects of the microstructure have been little considered in previous studies.

Morphology changes are also an important issue for these *quasi* one-dimensional materials when submitted to high-pressure conditions. Reduction in the aspect ratio can occur by fracture of these nanostructures at the moment of the phase transitions under hydrostatic compression conditions [11,17]. Eventually, morphology changes can also occur without modifications in crystalline structure, as observed for gallium nitride nanowires as reported by Dong et al. [18]. Therefore, the investigation of these materials under high-pressure conditions can provide valuable information about their compressibility, and morphological and structural stability.

Molybdenum oxide has several structural polymorphs depending on the thermodynamic conditions and it is a good model for investigating how the nanostructured form behaves when compared with the bulk counterpart. The orthorhombic phase (α-MoO_3) is thermodynamically stable and have a lamellar structure formed by asymmetrical MoO_6 octahedra coupled to each other through corner-linking along [100] and

---

* Corresponding authors.
E-mail addresses: jvaldenirs@fisica.ufc.br (J.V. Silveira), agsf@fisica.ufc.br (A.G. Souza Filho).

[1] Deceased.

https://doi.org/10.1016/j.saa.2017.11.053
1386-1425/

edge-sharing along [001]. Thus, stacked double-layer sheets parallel to the (010) plane are formed [Fig. 1(a)]. Weak van der Waals interactions between the double-layer sheets result in a zigzag chain with a unique layered structure. Furthermore, the monoclinic MoO_3-II phase also present corner- and edge-sharing MoO_6 octahedra, which form double-layer sheets parallel to the (010) plane. The main difference between the orthorhombic α-MoO_3 and the monoclinic MoO_3-II phases is the stacking sequence of the double-layers, which are defined by the position of the Mo atom relative to the O atoms in the MoO_6 octahedra. The stacking sequence in the orthorhombic α-MoO_3 phase is *aba*, whereas for the monoclinic MoO_3-II phase the sequence is *aaa* [Fig. 1(b)].

The orthorhombic α-MoO_3 phase has been prepared in a variety of novel morphologies, such as nanorods, nanobelts, and nanotubes [5,6,19]. Nanocrystalline α-MoO_3 has potential applications in various technologic fields, such as gas sensor, photodetector and waveguides for nanophotonics [19–21]. Microcrystalline α-MoO_3 under high-pressure conditions was studied by Liu et al. [22]. According to these authors, two phase transitions were found upon compression up to 43 GPa: the orthorhombic α-MoO_3 phase (space group *Pbnm*) changes to the monoclinic MoO_3-II phase (space group $P2_1/m$) at 12 GPa and subsequently to the monoclinic MoO_3-III phase (space group $P2_1/c$) at 25 GPa.

α-MoO_3 nanoribbons (NR), a typical *quasi* one-dimensional metal-oxide nanomaterial, exhibit distinct Raman bands behavior upon applying temperature compared with the α-MoO_3 bulk [23]. Although there are many reports of high-pressure studies of nanomaterials with different morphologies, to the best of our knowledge there are no reports for pressure-dependent investigations of such nanostructured MoO_3 materials.

In this work, we report a Raman spectroscopy study aiming to evaluate the crystalline structure behavior of α-MoO_3 nanoribbons under hydrostatic pressure in the range 0–21 GPa. The onset of the phase transition from the orthorhombic phase (α-MoO_3) to monoclinic phase (MoO_3-II) was observed at 5 GPa, which is quite lower compared to the corresponding bulk material (12 GPa) [22]. Furthermore, morphology changes of the α-MoO_3 nanoribbons were followed by Raman spectroscopy, which was also confirmed by *ex situ* scanning electron microscopy (SEM) analysis. Raman spectroscopy data suggest a strong pressure-induced morphological change and a decrease of the crystal size.

2. Material and Methods

MoO_3 nanoribbons were synthesized by using standard hydrothermal route as previously described [5,23]. Raman spectra were obtained in backscattering geometry by using a triple-grating spectrometer model T64000 (Jobin-Yvon) equipped with a nitrogen cooled CCD detector. An argon laser (514.5 nm) was used as excitation source. The laser power was set to 3 mW in order to avoid overheating of the sample. The slits were set for a spectral resolution of about 1 cm^{-1}. An Olympus microscope lens with a focal distance of 20.5 mm and a numerical aperture of 0.35 was used to focus the laser beam on the sample loaded in the pressure cell. High pressure Raman experiments were performed using two different diamond anvil cells. Nujol oil was used as pressure transmitting medium (PTM) in one cell which was able to operate in 0–10 GPa pressure range. The second diamond anvil cell, able to operate in 0–21 GPa pressure range, argon was used as PTM. This latter setup allows the sample recovery after the high-pressure cycle for subsequent SEM measurements. In both setups, the pressure values were estimated using the R_1 and R_2 ruby fluorescence lines shifts. The Raman bands characteristic (frequency and linewidth) were analyzed by fitting the spectra to a set of Gaussian and Lorentzian functions. SEM images were obtained using a field emission scanning electron microscopy (FE-SEM, NOVA 200 Nanolab, FEI Co.). Transmission electron microscopy (TEM) images were obtained using a Carl Zeiss CEM-902 operating at 80 kV.

3. Results and Discussion

Fig. 2(a) and (b) show, respectively, the TEM and SEM images of the as-synthesized α-MoO_3 nanoribbons (NRs). The MoO_3 NRs present a rectangular cross section resembling the “popsicle sticks” shape. The NRs present a few tens of nanometers thickness and high aspect ratio, with lengths up to a few microns and an average width of 200 nm [23]. Raman spectra recorded at room temperature and ambient pressure (Fig. 3–0.0 GPa) reveal typical signature of the orthorhombic α-MoO_3 phase (space group D_{16}^{2h}(*Pbnm*)) [24,25]. The well-defined Raman bands in the vibrational modes below 200 cm^{-1} indicate a very high degree of sample crystallinity. The stoichiometry of the NRs ($MoO_{2.94}$) was estimated by using an empirical model reported in literature [25].

Pressure dependent Raman measurements at room temperature are presented in Fig. 3 in frequency range between 1050 cm^{-1} and 80 cm^{-1}. The spectra intensities are normalized to the band intensity located at 816 cm^{-1} at ambient pressure. Based on group theory analysis 24 active Raman modes for α-MoO_3 phase ($8A_g + 8B_{1g} + 4B_{2g} + 4B_{3g}$) are expected. Raman spectra measured at ambient pressure (0.0 GPa) show 16 characteristic bands in good agreement with early reports [22–26]. Raman bands located at 993 cm^{-1} (A_g, antisymmetric $\nu_{as}M = O$), 816 cm^{-1} (A_g, symmetric $\nu_s M = O$), and 664 cm^{-1}(B_{2g}, B_{3g}, antisymmetric ν_{as}O–M–O) are stretching modes. Notwithstanding, bands located at 467 cm^{-1} (A_g, δO–M–O bend), 378 cm^{-1} (A_g, B_{1g}, δO–M–O scissor), 336 cm^{-1} (A_g, δO–M–O scissor), 290 cm^{-1} (B_{3g}, $\delta O = M = O$ wagging), 280 cm^{-1} (B_{2g}, $\delta O = M = O$ wagging), 249 cm^{-1} (B_{3g}, $\tau O = Mo = O$ twist) and 197 cm^{-1} (B_{2g}, $\tau O = Mo = O$ twist) are assigned as deformation modes. Lastly, the observed bands located at 219 cm^{-1} (A_g, rotational rigid MoO_4 chain mode, R_c), 160 cm^{-1} (A_g/B_{1g}, translational rigid MoO_4 chain mode, T_b), 127 cm^{-1} (B_{3g}, translational rigid MoO_4 chain mode, T_c), 116 cm^{-1} (B_{2g}, translational rigid MoO_4 chain mode, T_c), 99 cm^{-1}(B_{2g}, translational rigid MoO_4 chain mode, T_a), and 78 cm^{-1} (A_g, translational rigid MoO_4 chain mode, T_a) are lattice modes [26].

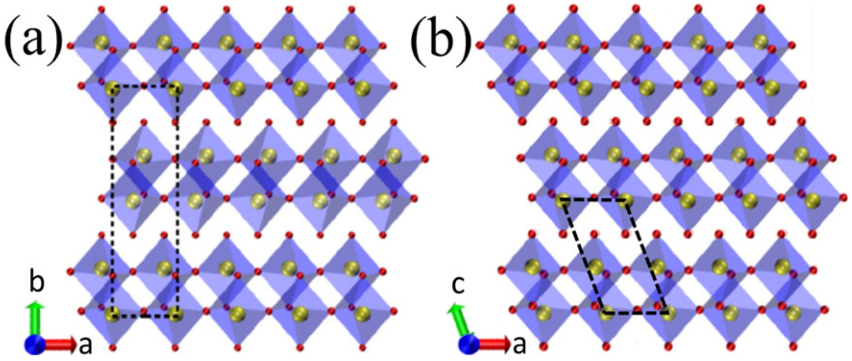

Fig. 1. MoO_6 octahedra sharing corners and edges in double-layers arrangements (a) *aba* stacking for orthorhombic α-MoO_3 and (b) *aaa* stacking for monoclinic MoO_3-II phase.